

Turbulence Effect on Gas Transport in Three Contrasting Forest Soils

Martin Maier*

Helmer Schack-Kirchner

Institute of Soil Science and Forest Nutrition
Univ. of Freiburg
79085 Freiburg im Breisgau, Germany

Marc Aubinet

Stéphanie Goffin

Unité de Physique des Biosystèmes
Faculté Universitaire des Sciences Agronomiques de Gembloux
5030 Gembloux, Belgium

Bernard Longdoz

Florian Parent

Unité d'Ecophysiologie forestière
INRA Centre de Nancy
F54280 Champenoux, France

Atmospheric turbulence can affect soil gas transport, and thus violates the assumption that molecular diffusion is the only relevant transport mechanism in the soil. Due to the oscillating character of turbulence-induced pressure pumping the net vertical air flow into/out of the soil is zero. Yet, the dispersion processes induced by the oscillating air movement in the soil pores enhance the gas exchange in the soil, and should be considered when the gradient method is applied. We developed a simple lab method to test the impact of turbulence-driven pressure pumping on soil gas transport using neon as a tracer gas. The experiment was conducted using soil core samples from three contrasting forest sites. The ratio of air permeability and air-filled pore-volume, k_a/ε , was found to be suitable to assess the sensitivity of soil gas transport to the pressure-pumping effect. The pressure-pumping effect reached up to 60% of the diffusive flux rates depending on the intensity of pressure pumping. We conclude that the turbulence effect can substantially influence soil gas transport in field studies, especially at sites with a high k_a/ε value $>1000 \mu\text{m}^2$. Therefore, we recommend taking this effect into account when soil gas flux is determined using the gradient method.

Abbreviations: α , dispersivity; C_{out} , neon concentration at the chamber outlet; ε , air-filled pore-space; D_0 , diffusion coefficient in air; D_{disp} , dispersion term; D_{disp}/D_0 , relative dispersion coefficient; D_{res} , resulting diffusivity; D_S , effective gas diffusion coefficient, D_S/D_0 , relative diffusion coefficient; k_a , air permeability, κ_p , pressure diffusivity; η , viscosity of the air; p , pressure fluctuations; P_0 , mean atmospheric pressure; v , gas velocity.

The production of CO_2 in the soil by roots, microorganisms, and macrofauna not only varies temporally and spatially on the plot and the landscape level, but also vertically with soil depth. Using chamber techniques it is possible to address the spatial and the temporal variation of the CO_2 efflux at a site. However, it is impossible to gain information about the vertical distribution of CO_2 sources within the soil profile, which is important to improve our understanding of the influence of parameters varying with depth. The gradient method (DeJong and Schappert, 1972; Davidson et al., 2006; Massman, 2006; Pumpanen et al., 2008; Schack-Kirchner et al., 2011) could potentially overcome this limitation. Although the main gas transport process in soils is diffusion, advection can be important under certain circumstances such as large changes in barometric pressure (Clements and Wilkening, 1974; Elberling et al., 1998), a rising ground water table (Jiao and Li, 2004; Maier et al., 2010), or wind-induced stationary pressure differences across topographical features (Amos et al., 2009; Bowling and Massman, 2011). This advective contribution can be integrated in the gradient method using a suitable gas transport model (e.g., Fang and Moncrieff, 1999). The

Soil Sci. Soc. Am. J.
doi:10.2136/sssaj2011.0376
Received 4 Nov. 2011.

*Corresponding author (martin.maier@bodenkunde.uni-freiburg.de)

© Soil Science Society of America, 5585 Guilford Rd., Madison WI 53711 USA

All rights reserved. No part of this periodical may be reproduced or transmitted in any form or by any means, electronic or mechanical, including photocopying, recording, or any information storage and retrieval system, without permission in writing from the publisher. Permission for printing and for reprinting the material contained herein has been obtained by the publisher.

major challenge here is the measurement of the pressure gradient, which can be hardly detectable (Maier et al., 2010).

In addition to these static pressure gradients, resulting from low-frequency pressure changes (time scale of hours to days), there are also high-frequency pressure fluctuations (>0.1 Hz) due to atmospheric turbulence. Field studies showed that these high-frequency pressure fluctuations can strongly influence soil gas concentrations (Hirsch et al., 2004; Seok et al., 2009; Flechard et al., 2007, Maier et al., 2010), and hence also soil gas transport and efflux. It is important to note that high-frequency pressure fluctuations do not induce a persisting pressure gradient as wind with laminar flow over topographical features does. If laminar wind is flowing steadily, for example, over a rock pile, a persistent pressure difference between the upwind to the downwind side can result in a continuous air flow through the porous pile (Amos et al., 2009). But in the case of a flat but complex surface, such as a plain covered by forest, wind will only induce turbulent flow with oscillating pressure fluctuations, and the net air flow into or out of the soil is zero. Nevertheless the observed effect on soil gas concentrations occurs throughout the entire profile (Seok et al., 2009; Maier et al., 2010). The pressure pumping induces an oscillating flow in the soil pores that seems to “enhance the diffusion” of the soil gas. This effect of turbulence-driven pressure pumping can be attributed to dispersion processes (Take et al., 2004).

Fukuda (1955) theoretically examined the movement of air in soil due to “wind gustiness”. Some years later, Scotter and Raats (1968) presented results from an experiment using a piston to impose a small sinusoidal movement on the air in a cylinder packed with sand. They observed an enhancement of gas exchange through the sand cores, and thus could clearly demonstrate the importance of the dispersion effect due to oscillating air flow. Recent research about gas dispersion in the soil focused on the dependence of dispersivity on substrate type (Hamamoto et al., 2009; Gidda et al., 2006; Sharma and Poulsen, 2010). The set-up used in these experiments is designed to accurately determine the dispersion induced by continuous gas flow and not by oscillating gas flows. To model the transport of contaminants, for example, by soil vapor extraction, these measurements are close to reality. Yet, this standard method (e.g., Hamamoto et al., 2009) does not allow relating the driving force (turbulence), the oscillating flow due to pressure pumping, and the effect of “enhanced diffusion”.

Modeling CO_2 flux in a snowpack, Massman and Frank (2006) integrated diffusion, viscous flow, and also dispersion into the gradient method. Based on modeling with synthetic pressure-pumping data, Poulsen and Møldrup (2006) also emphasized the importance of pressure pumping and addressed the crucial role of soil physical parameters on soil-atmosphere gas exchange. There are several transfer functions available that can be used to derive the parameters that are difficult to measure, for example, the diffusion coefficient D_s , from parameters that can be easily determined, for example, the air-filled pore-volume (Millington, 1959; Møldrup et al., 1999). Yet, these functions are not able to fully reflect site-specific factors, which can be crucial if the relevance of pressure pumping must be evaluated for different sites.

In this paper (i) we discuss the transport mechanisms underlying the turbulence-driven pressure pumping and present a conceptual model. We propose to integrate the pressure-pumping induced dispersion and the diffusion as “apparent diffusion”, which easily could be used in field studies applying the gradient method. (ii) We examine the effect of pressure pumping on gas transport through undisturbed soil samples from three sites using a new experimental design. The experimental data are analyzed to evaluate the impact of relevant soil physical parameters on the sensitivity of soil gas transport to pressure pumping. The laboratory results help us to assess the sensitivity of the soil to the pressure-pumping effect at the three forest sites where the gradient method is currently applied.

TURBULENCE-DRIVEN PRESSURE PUMPING

The amplitudes of high-frequency pressure fluctuations are very small compared to the barometric pressure. Hence, the vertical air flow into/out of the soil is very small compared to the depth of a soil (a pressure fluctuation of 10 Pa can compress the soil air column by 0.1 mm, if a barometric pressure of 100 kPa and a soil depth of 1 m is assumed). Though, the movement of the soil air column can be substantial compared to the diameter of the soil pores. As a result of the alternating direction of the pressure fluctuation, the net vertical air flow into/out of the soil is zero, although air flow occurs within the soil pores.

The effect of turbulence-driven pressure pumping on soil gas transport can be basically explained by dispersion induced by the oscillating airflow in the soil pores. The phenomenon of dispersion is well-known, for example, from contaminant transport in ground water (Delgado, 2006), but is also relevant in the gas phase of porous media (Scotter and Raats, 1969; Costanza-Robinson and Brusseau, 2002).

Generally, the dispersion in soil pores can be attributed to molecular diffusion and mechanical mixing components. Figure 1 visualizes the gas transport in a soil pore driven only by diffusion (left), and additionally driven by pressure pumping (middle: downward movement of the soil air column; right: upward movement). The enhancement of the gas transport due to pressure pumping can be mainly explained by three effects.

First, dead-end pores do not contribute to the gas transport under calm conditions, and there is no concentration gradient between dead-end pore and main pore (Fig. 1 left: A). But when the air column is oscillating, the vertical concentration gradient in the main pore results in an additional, lateral concentration gradient between the dead-end pore and the main pore with oscillating direction (Fig. 1 middle, right: A). When the air column in the main pore is below the neutral point, the lateral concentration gradient leads to diffusion of CO_2 molecules into the main pore (Fig. 1 middle: A). When the air column is above the neutral point (that means air from a deeper position and a higher CO_2 concentration is shifted upward in the main pore), the CO_2 molecules diffuse from main pore into the dead-end pore, “loading” the dead-end pore with CO_2 (Fig. 1 right: A). Thus, the oscillating air acts as a “ladder”.

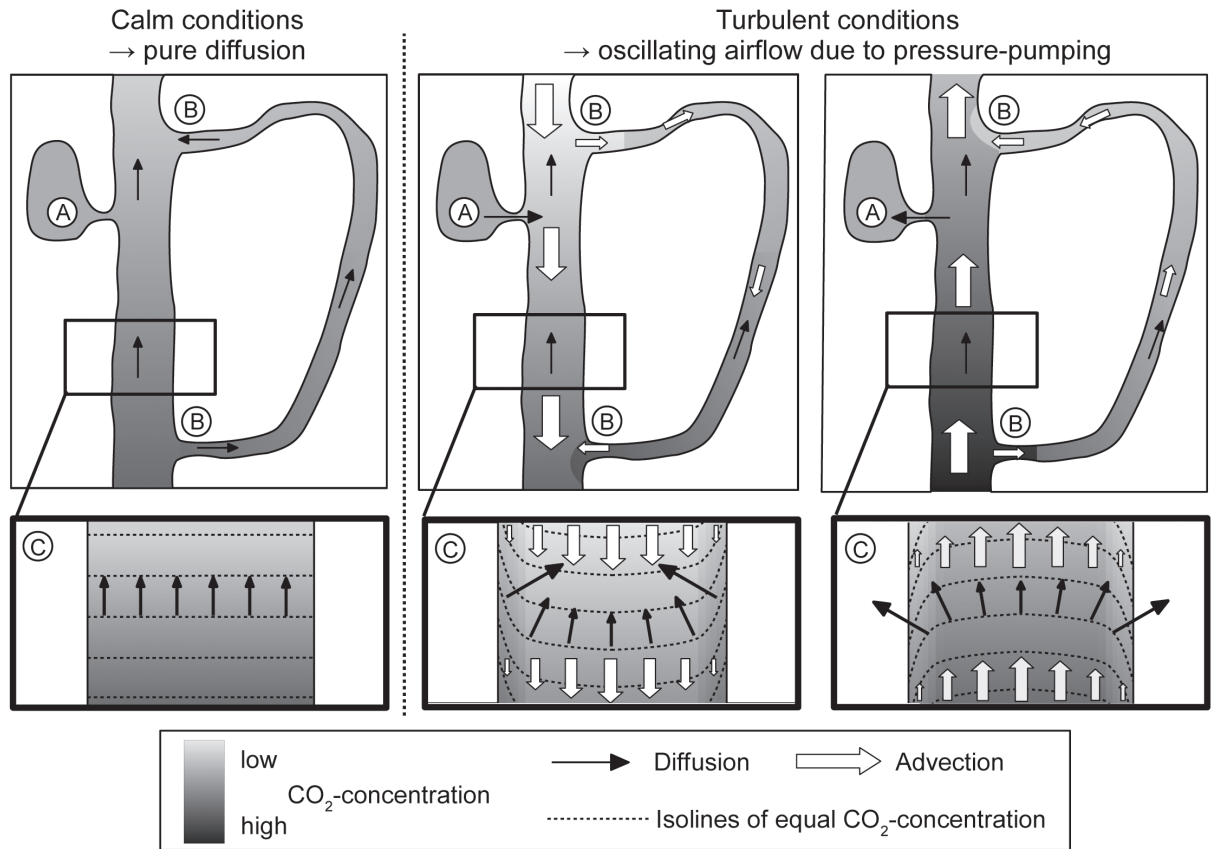


Fig. 1. Soil gas transport under calm and under turbulent conditions including diffusion, advection, and dispersion.

Second, there is mechanical mixing of soil air at the intersection of pores (Fig. 1 middle, right: B). Because of different permeability, the flow rate of air differs between the soil pores leading to horizontal concentration heterogeneity, and finally to an irreversible mixing of air with different CO_2 concentrations.

Third, even within a single pore the gas velocity differs depending on the distance to the pore wall due to wall friction. As a consequence the concentration isolines, which are straight under calm atmospheric conditions, become curved under turbulent conditions due to pressure pumping (Fig. 1:C). When the oscillating air column is below the neutral point, the CO_2 molecules close to the wall diffuse toward the center of the pore (Fig. 1 middle: C) and are then transported upward. As soon as the air column is above the neutral point, the direction of the diffusion is reversed toward the pore wall by diffusion (Fig. 1 right: C). Therefore the CO_2 molecules preferentially use the upward movement of the oscillating air column.

Theoretically, in a vertically homogeneous soil, gas transport can be calculated using the advection–diffusion–dispersion equation:

$$\frac{\partial C}{\partial t} = (D_S + \alpha |v|) \frac{\partial^2 C}{\partial z^2} - v \frac{\partial C}{\partial z} + S \quad [1]$$

where C is the concentration of the gas species ($\mu\text{mol mol}^{-1}$), t is time (s), D_S is the gas diffusion coefficient in the soil ($\text{m}^2 \text{s}^{-1}$), α is the dispersivity (m), z is the depth (m), S is the source term ($\mu\text{mol mol}^{-1} \text{s}^{-1}$), and v (m s^{-1}) is the vertical velocity of the air-flow. The dispersion coefficient D_{disp} ($\text{m}^2 \text{s}^{-1}$) is the product of α

and v , $D_{\text{disp}} = \alpha |v|$, where v is an absolute value because dispersion happens in both directions and is always positive. If we apply Eq. [1] to the turbulence-driven pressure pumping on a time scale larger than 5 min, the mean of v becomes zero, because of the oscillating character of the flow. Hence, the advective contribution to the gas transport is zero. However, the instantaneous gas velocity and thus the mean absolute value of v is not zero and we have to consider dispersion. It is D_{disp} that represents the pressure-pumping effect, which we want to integrate in the modeling of field studies. We define the sum of the diffusion and dispersion coefficients as the resulting exchange coefficient D_{res} ($\text{m}^2 \text{s}^{-1}$): $D_{\text{res}} = D_S + D_{\text{disp}}$. Hence, the pressure-pumping induced dispersion effect can be dealt with as an additive term in the regular diffusion equation using D_{res} instead of D_S .

The dispersivity α mainly depends on the geometry of the air-filled pores (Costanza-Robinson and Brusseau, 2002; Sharma and Poulsen, 2010), while the mean $|v|$ depends on the characteristics of the pressure fluctuation at the surface and the physical properties of the soil (Poulsen and Møldrup, 2006). The $|v|$ value at a depth is linked to the penetration of pressure fluctuations p (Pa) into the soil that can be obtained using (Fukuda, 1955):

$$\frac{\partial p}{\partial t} = \kappa_p \frac{\partial^2 p}{\partial z^2} \quad [2]$$

Equation [2] is a diffusion-like equation, in which the pressure diffusivity κ_p ($\text{m}^2 \text{s}^{-1}$) is described by:

$$\kappa_p = \frac{k_a P_0}{\varepsilon \eta}, \quad [3]$$

where k_a is air permeability (μm^2), ε is air-filled pore-volume ($\text{m}^3 \text{m}^{-3}$), P_0 the mean atmospheric pressure (Pa), and η is the viscosity of the air ($\mu\text{Pa s}^{-1}$). While P_0 and η represent the influence of the fluid, k_a and ε reflect the dependence on physical soil properties. A higher k_a/ε ratio (μm^2) results in higher pressure diffusivity, and thus an easier and deeper penetration of pressure fluctuations into the soil.

Based on Eq. [1–3] and Darcy's law, Massman (2006) calculated the resulting three-dimensional pressure field and gas velocity v for a layered medium. The resulting equations were used to derive reference values of D_{disp} for our laboratory experiment results. However, this physically-based model needs many input parameters that are difficult to obtain in the field.

MATERIALS AND METHODS

Description of the Sites

Three different forest sites (Hartheim, Germany; Hesse, France; Vielsalm, Belgium) were chosen to take undisturbed soil core samples at different depths. A meteorological tower is present at each experimental site to measure the main meteorological variables including wind speed and friction velocity. The three sites differ largely in their stand characteristics and soil properties (Table 1). The Scots pine stand at the Hartheim site has a sparse canopy and a dense understory, while the beech stand at Hesse and the mixed stand at Vielsalm have a dense canopy and no understory. The soil at Hartheim has a high porosity and is well aerated, while porosity and aeration at Vielsalm are reduced due to soil compaction. At Hesse the aeration of the topsoil is intermediate, but the subsoil shows stagnant properties.

Table 1. Description of the experimental forest sites Hartheim (Germany), Hesse (France), and Vielsalm (Belgium). Soils were classified according USDA (Soil Survey Staff, 2006) and WRB classification (FAO, 2006).

Site	Hartheim	Hesse	Vielsalm
Location	Upper Rhine Valley/47°56' N, 7°36' E	Northeast France/ 48°40' N, 7°05' E	Belgian Ardennes/ 50°18' N, 6°00' E
Elevation above sea level	200 m	300 m	450 m
Mean annual temperature	10.3°C†	9.2°C‡	7.0°C§
Mean annual precipitation	642 mm†	820 mm‡	1000 mm§
Soil type USDA	Calciudoll	Hapludalf	Dystrudept
Soil type WRB	Haplic Regosol	Stagnic Luvisol	Haplic Cambisol
Texture	Silt loam (topsoil), sand and gravel (subsoil)	Silt loam	Silty clay loam
Available water capacity	80 mm (0–0.6-m depth)¶	175 mm (0–1.6-m depth)‡	150 mm (0–0.6-m depth)
pH _{H2O}	7.8–8.2¶	4.9	3.7–4.5
Organic carbon	14.20 kg m ⁻² ¶	10.07 kg m ⁻² ‡	9.44 kg m ⁻²
Humus type	Mull	Moder	Moder
Tree species	Scots pine (<i>Pinus sylvestris</i> L.)	European beech (<i>Fagus sylvatica</i> L.)	Mixed stand dominated by European beech
Stand height/age	14 m/45 yr†	16.2 m/30 yr‡	27 m/100 yr††
Diameter at breast height	0.19 m†	0.10 m‡	1.06 m††
Stand density	800 trees ha ⁻¹ †	2600 trees ha ⁻¹ ‡	243 trees ha ⁻¹ ††

† Holst et al. (2008).

‡ Granier et al. (2008).

§ Aubinet et al. (2005).

¶ Maier et al. (2010).

Granier et al. (2000).

†† Aubinet et al. (2001).

Standard Measurements of Soil Physical Parameters

For the standard measurements of soil physical parameters (porosity, water retention characteristics, diffusivity, and air permeability) we took 127 undisturbed 200 cm³ core samples (5 cm height) at different depths at the different sites. The porosity of the soil samples was determined by vacuum pycnometry and the thermogravimetric method (Hartge and Horn, 1999). To obtain the water retention curves the samples were saturated with water and then successively drained applying defined levels of water potential using a filter bed and a pressure plate.

Gas diffusivity (D_G) was measured at different levels of water potential employing a nonstationary one-chamber method (Kühne et al., 2011), using neon as a tracer gas. The intact soil cores were placed on top of a chamber, so that gas exchange was restricted to diffusion through the soil sample. A defined amount of neon was injected into the chamber. From the decreasing neon concentration over time the diffusivity D_G and the dimensionless relative diffusivity D_G/D_0 were determined.

Air permeability was measured with a device similar to that described by Iversen et al. (2001), where air flows through a soil ring sample at a constant rate. The pressure gradient across the soil sample at a given flow rate is inversely proportional to the air permeability. The device was equipped with a highly sensitive pressure sensor (GMSD 2.5 MR, 125 Greisinger Electronic GmbH; Regenstauf; Germany; sensitivity 0.1 Pa). For each site the horizon-specific dependence of diffusivity and air permeability on air-filled pore volume was derived using nonlinear regression functions.

Turbulence Experiment

We developed a steady-state method to measure the resulting soil gas diffusivity, which could also be used to test the effect of turbulence-

driven pressure pumping on gas transport. The set-up was similar to that of Jassal et al. (2005). The method was modified using a peristaltic pump and neon as a tracer gas. A soil core sample (200 cm³) was fixed on top of an open-top chamber (200 cm³), through which air with a defined concentration of tracer gas was circulated. This air entered at the bottom of the chamber with a constant neon concentration of 0.1% (Fig. 2, side view). A perforated tube positioned right below the soil sample collected the air leading it to a micro-gas chromatograph (CP2002P, Chrompack, Middelburg, the Netherlands, CP-Molsieve-5A column, helium as carrier gas). The flow rate into and out of the chamber was exactly the same and was controlled by a peristaltic pump. The loss of neon was restricted to diffusion through the soil sample (when turbulence above the sample is zero). After a certain time, an equilibrium situation is established and a stationary neon concentration in the chamber will be reached. No fan was located inside the chamber to avoid undesired turbulence. In this stationary situation, the tracer gas flux through the soil sample (F , m³ s⁻¹) corresponds only to diffusion and dispersion because the source and the advective terms are zero, leading to the following equation:

$$F = (D_S + D_{\text{disp}}) \frac{\partial C}{\partial z} = D_{\text{res}} \frac{\partial C}{\partial z}, \quad [4]$$

Thus, D_{res} (m² s⁻¹) could be calculated by

$$D_S + D_{\text{disp}} = D_{\text{res}} = \frac{F}{\Delta C / \Delta z} = \frac{\Phi (C_{\text{in}} - C_{\text{out}})}{(C_{\text{out}} - C_{\text{atm}}) / h}, \quad [5]$$

where Φ is the flow rate of the pump (m³ s⁻¹), C_{in} , C_{out} and C_{atm} the neon concentration ($\mu\text{mol mol}^{-1}$) at the chamber inlet, outlet and in the atmosphere, and h the height of the soil sample (m).

The set-up allowed us to measure five samples simultaneously (Fig. 2, top view). To simulate a flat soil surface, the soil rings were mounted into a panel, so that the panel surface and the top of the soil samples formed a plane surface (Fig. 2, side view). This was necessary to avoid local effects and to ensure that all five samples received the same turbulence-induced pressure fluctuations. Turbulence was generated by a constantly blowing fan and a slowly turning chopper wheel. The resulting air movement across the experimental surface varied continuously, inducing pressure fluctuation at the samples

surfaces. To assess the pressure pumping two of the chambers were equipped with a sensor (GMSD 2.5 MR, Greisinger Electronic GmbH; Regenstauf, Germany) to measure the pressure fluctuations. The atmospheric turbulence was measured at 10 Hz using a sonic anemometer (81000V, R. M. Young Company, Traverse City, MI) installed in front of the experimental set-up.

At first, the diffusivity of the soil samples was measured under calm conditions where pressure pumping had no effect ($D_{\text{res}} = D_S$). Then the turbulence generator was switched on (= turbulence Level 1) and a new steady state was reached. Then a higher turbulence level (= turbulence Level 2) was set. The difference between D_{res} measured under calm conditions (= D_S) and D_{res} measured under turbulent conditions could be attributed to turbulence-induced dispersion (D_{disp}). Analogous to D_S/D_0 , we define the dimensionless relative dispersion coefficient D_{disp}/D_0 and the relative resulting exchange coefficient D_{res}/D_0 .

For this experiment we used five topsoil samples (0–5-cm depth) of each site at two different soil moisture levels. The friction velocity u^* (m s⁻¹) was used as a proxy specifying the turbulence intensity (Stull, 1988). The friction velocity is obtained from $u^* = \sqrt{-(\overline{u'w'})}$ where u' and w' are the fluctuations of the horizontal and vertical wind velocities compared to the mean values (m s⁻¹), respectively, and $(\overline{u'w'})$ represents the temporal mean value of the product of u' and w' .

All statistical analyses were accomplished using the software SAS 9.2 (SAS Institute Inc., Cary, NC). We used the procedure PROC NLIN for nonlinear curve-fitting. To smooth the water retention curve the procedure PROC TPSPLINE was used. The effect of turbulence-driven pressure pumping on D_{res}/D_0 was tested at $p = 0.05$ using the Friedman test.

RESULTS

Pore-Size Distribution, Diffusivity, and Air Permeability

The pore-size distribution was derived from the measured soil-water retention curves, assuming radial pore geometry. At Hartheim the soil is well aerated throughout the profile, and has a large volume of macropores representing interaggregate pores (Fig. 3a). At Hesse the profile was slightly compacted in the top soil (depth <25 cm).

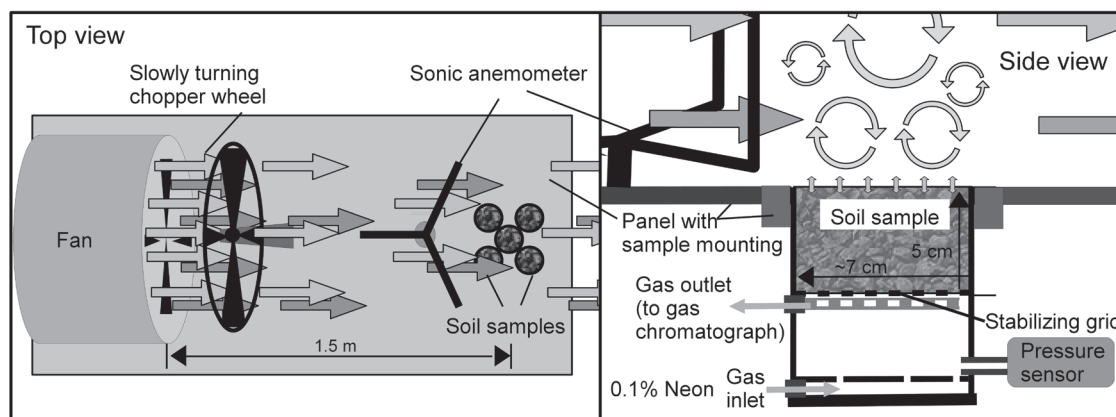


Fig. 2. Set-up of a steady-state method to measure the soil gas diffusivity under calm and the resulting soil gas diffusivity under turbulent conditions. The flow rate of the gas into and out of the chamber was controlled by a peristaltic pump.

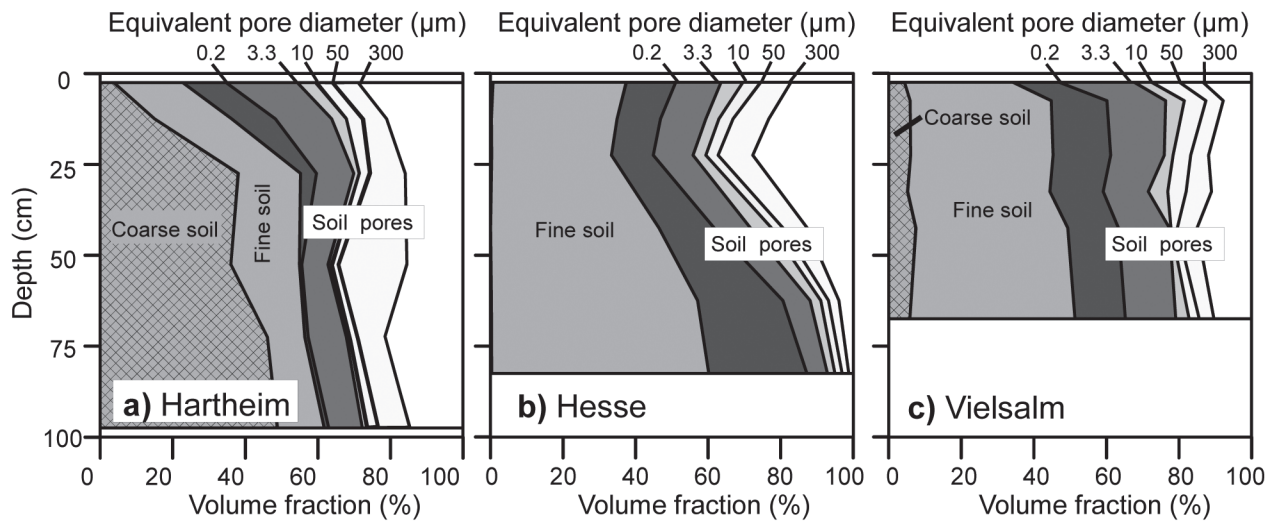


Fig. 3. Profiles of the pore-size distribution at the experimental sites. Equivalent pore diameter was derived from matric potential.

The volume of the macropores (diameter $>300 \mu\text{m}$) diminishes at depth $>60 \text{ cm}$, so aeration of the subsoil is limited (Fig. 3b). At Vielsalm traces of compaction due to the use of forestry machinery were visible in the field. Here, also the volume of the macropores ($>300 \mu\text{m}$ diam.) in the top soil was lowest (Fig. 3c).

The topsoil (0–5 cm) at all sites revealed distinct relationships between ε and D_S/D_0 (Fig. 4a, 4b, and 4c). At similar ε values the Vielsalm samples generally had the lowest D_S/D_0

D_0 values. The relationship between k_a and ε was more scattered (Fig. 4d, 4e, 4f), especially for the Hartheim samples where the highest k_a values were observed. As the pore-volume decreases with soil depth, the measured D_S/D_0 and k_a values decreased with depth (data not included).

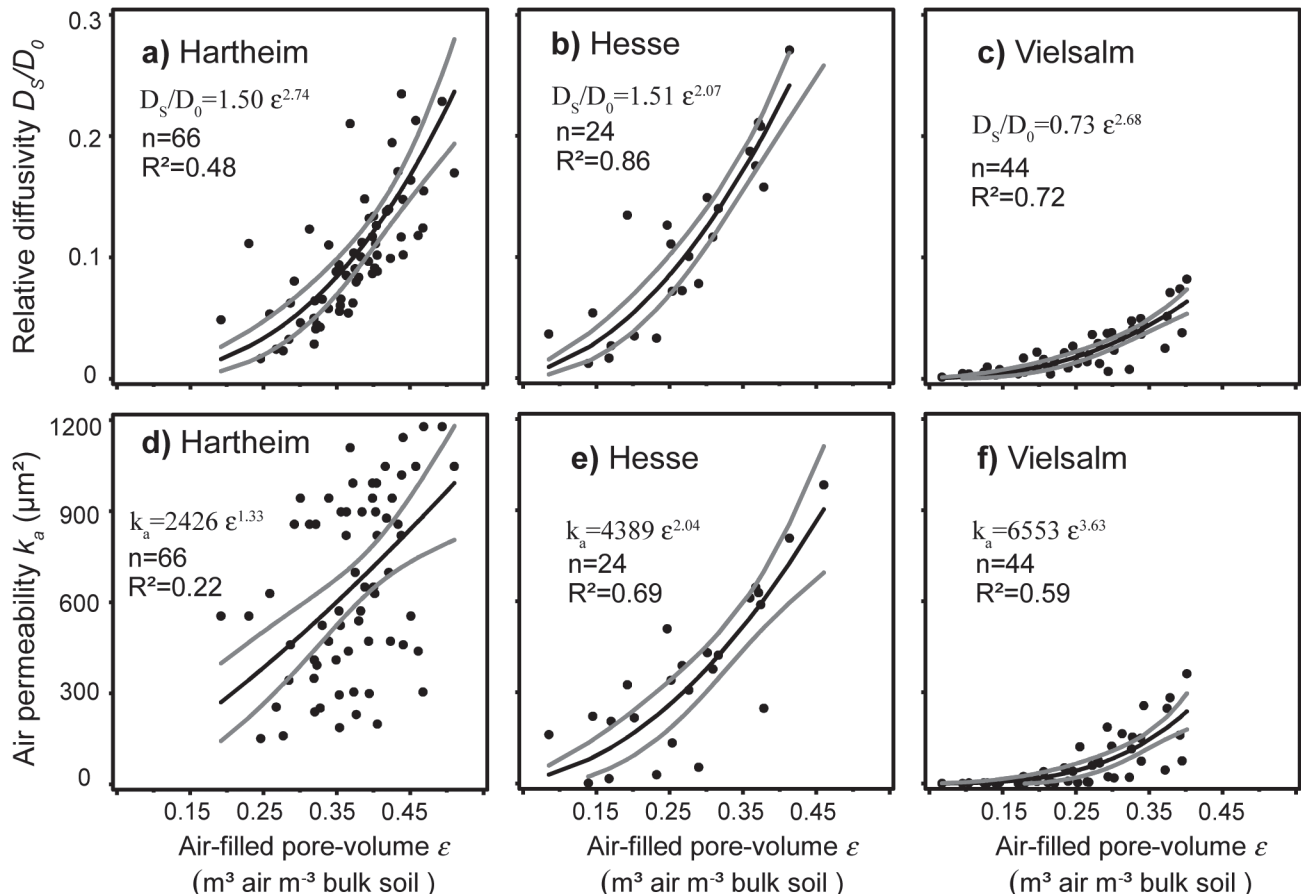


Fig. 4. (top) Relationship between the relative diffusion coefficient D_S/D_0 and the air-filled pore-volume ε and (bottom) relationship of air permeability k_a and ε of topsoil samples (0–5-cm depth).

Turbulence Experiment

The results of a demonstration test are plotted in Fig. 5. For this run, five plastified soil samples with similar air-filled pore-volume, but distinct effective gas diffusion coefficient and air permeability were used (Fig. 5a, see legend). The soil physical properties of the samples were non-natural due to the plastification. Yet, the underlying physical principle of the pressure-pumping effect could clearly be observed on these samples. When a steady-state concentration was reached the turbulence generator was switched on (Fig. 5b) to start turbulence-driven pressure pumping. As a result the neon concentration in the chamber (C_{out}) dropped substantially in some of the chambers and tended to a new steady-state concentration. D_S was calculated from the steady-state concentration under calm conditions, where a high concentration corresponds to a low value for D_S (see Eq. [5]). The decrease in the steady-state C_{out} concentration under turbulent conditions due to the pressure-pumping effect did not depend on the initial D_S value, but rather on k_a (see Fig. 5a). Only samples with high air permeability

showed a substantial decrease in the steady-state concentration under turbulent conditions (Fig. 5a: samples 1, 2, and 5).

Unfortunately the peristaltic pump used in the experiment induced a small oscillating pressure fluctuation in the chamber. The pressure fluctuations induced by the pump were tested by sealing the chambers with solid plastic samples and were the same for all chambers. The resulting pressure fluctuations were less but still detectable when soil samples were fixed on the chambers (Fig. 5c, 5d, turbulence Level 0). Samples with a higher k_a/ε -value revealed lower basic pressure fluctuations, because the pressure fluctuations induced by the peristaltic pump could easily “be transported” through the sample to the atmosphere. This caused probably an overestimation of D_S . Nevertheless, the conclusions drawn for turbulence-induced D_{disp} remain unchanged, because this effect was the same at all turbulence levels.

The mean value of the friction velocity u^* was $<0.01 \text{ m s}^{-1}$ under calm conditions, 0.17 m s^{-1} at turbulence Level 1, and 0.34 m s^{-1} at turbulence Level 2. The turbulence-driven pressure fluctuations at the surface of the different soil samples were the same at a given turbulence level. Yet, the penetration of pressure

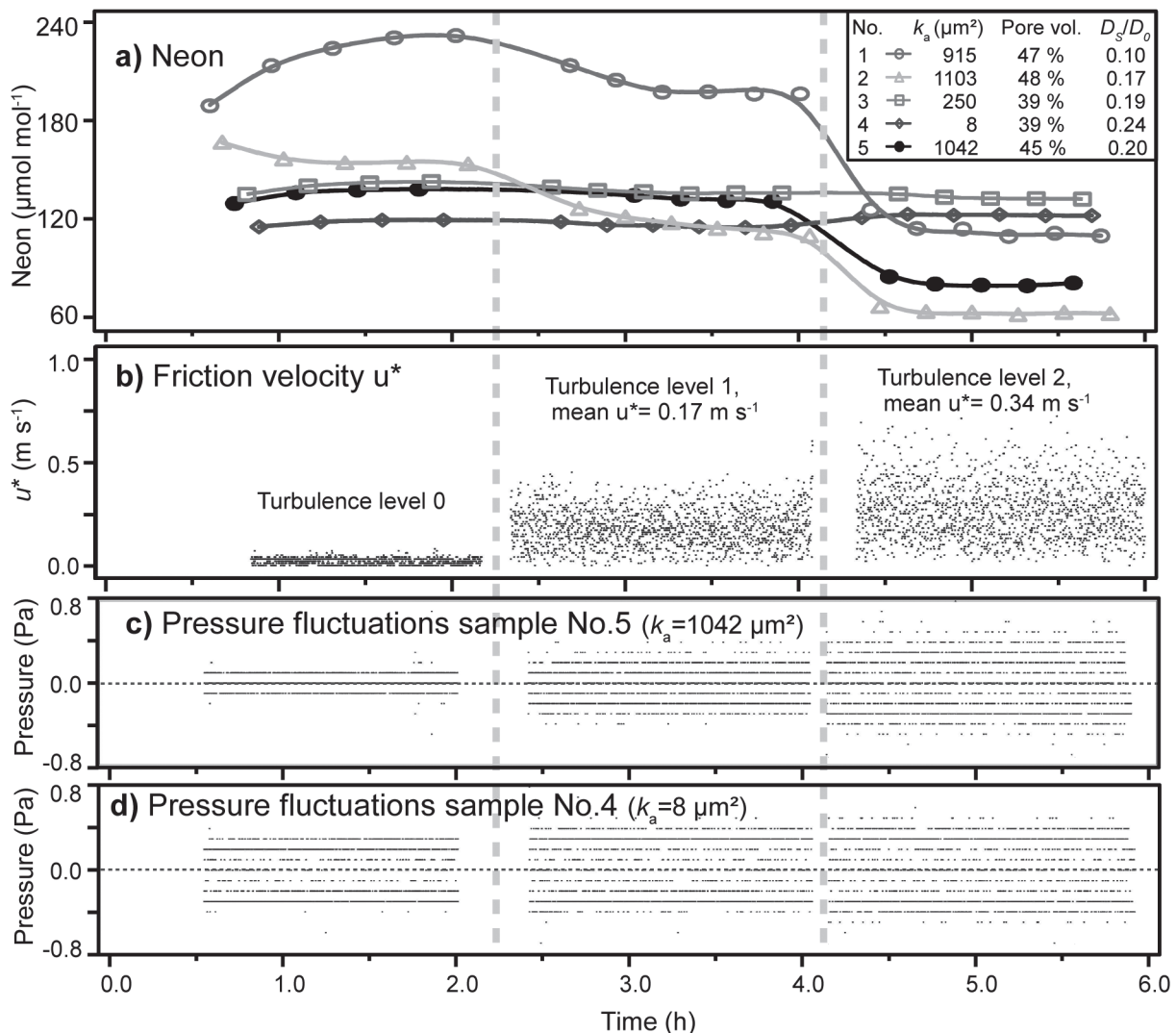


Fig. 5. Test results using plastified soil samples. Time series of (a) the resulting steady-state concentrations of neon in the chamber, (b) friction velocity u^* , and (c, d) pressure fluctuations within the respective chamber.

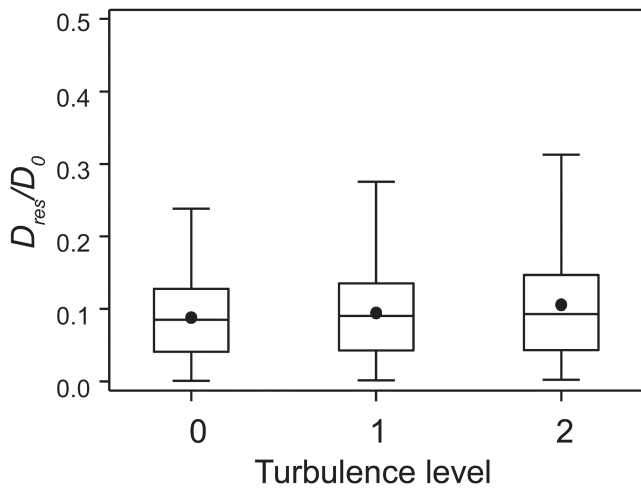


Fig. 6. The relative resulting exchange coefficient D_{res}/D_0 at different turbulence levels. The boxes indicate 25th, 50th, and 75th percentiles, the dot the mean value.

fluctuations through the samples depends on the pressure diffusivity, and thus the resulting pressure fluctuation in each chamber was different. The observed pressure fluctuation in the chambers increased with increasing turbulence (Fig. 5c, 5d). This response was stronger for the soil sample with the higher k_a (Fig. 5c). The turbulence induced pressure fluctuations in the chambers (excluding the basic fluctuations) increased by 100% when changing from turbulence Level 1 to Level 2. Thus, an increase by 100% of the turbulence-induced pressure fluctuations at the sample surface was assumed.

The relative resulting exchange coefficient D_{res}/D_0 at a given turbulence level varied widely due to the distinct soil characteristics and the large range in soil moisture of the measured samples (Fig. 6). A statistically significant increase in D_{res}/D_0 with increasing turbulence level was obtained using the Friedman test (nonparametric statistical test for paired measurements, $p = 0.05$).

To focus on the effect of pressure pumping only D_{disp}/D_0 was considered. To analyze the effect of soil physical parameters on D_{disp}/D_0 at a given turbulence level, we tested different parameters. The ratio of air permeability and air-filled pore space (k_a/ϵ) was the best explanatory variable (Fig. 7). D_{disp}/D_0 increased with k_a/ϵ . Indeed, as this parameter combination describes the soil physical component of the pressure diffusivity, it is able to explain a part of the D_{disp}/D_0 variation between the samples ($R^2 = 0.48$ at turbulence Level 1, $R^2 = 0.38$ at turbulence Level 2). The experimental relationship was compared to modeled ones obtained from Eq. [9] of Massman (2006) who modeled the air-flow velocity in the soil pores to derive D_{disp} (Fig. 7). To run the model for a situation similar to turbulence Level 1 (Level 2), a pressure fluctuation of 0.5 Pa (1 Pa, respectively), and a wave frequency of 1 Hz were used (values in agreement with the observed increase of pressure fluctuations in the chambers, Fig. 5c, 5d). For the dispersivity α different realistic values were used (Hamamoto et al., 2009).

To compare the importance of the pressure-pumping induced dispersive transport to normal diffusion D_{disp} was divided by D_S . The dispersive transport D_{disp} reached up to 15% at turbulence Level 1, where no clear relationship between D_{disp}/D_S and other soil physical parameter could be found (including k_a/ϵ , Fig. 8a). At turbulence Level 2, D_{disp}/D_S reached up to 85% (probably an outlier, Fig. 8b). Samples with a $k_a/\epsilon > 1000 \mu\text{m}^2$ showed substantially higher D_{disp}/D_S values. Single samples showed no turbulence effect, or even a small reduction in D_{res} , that caused negative values of D_{disp} to be estimated (Fig. 7). These values become more negative when they are divided by a (low) D_S value (Fig. 8). We attribute these negative D_{disp}/D_S values, and also the extreme high outlier, to measurement uncertainty.

Relevance for Sites

The results of the turbulence experiment proved that k_a/ϵ has an important effect on D_{disp} . Thus, we used it as surrogate to determine the sensitivity of the soil gas transport to pressure pumping on a larger data set from our three experimental sites.

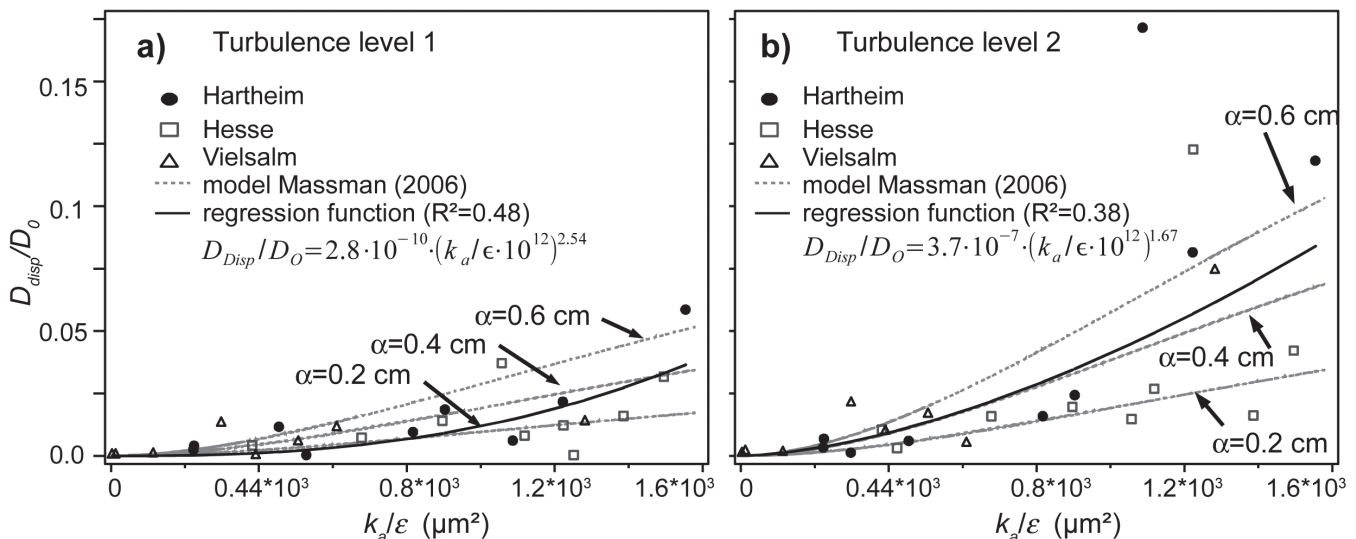


Fig. 7. Relationship between the pressure-pumping effect (measured as the dimensionless relative dispersion coefficient D_{disp}/D_0) and the parameter combination k_a/ϵ for (a) turbulence Level 1 and (b) turbulence Level 2.

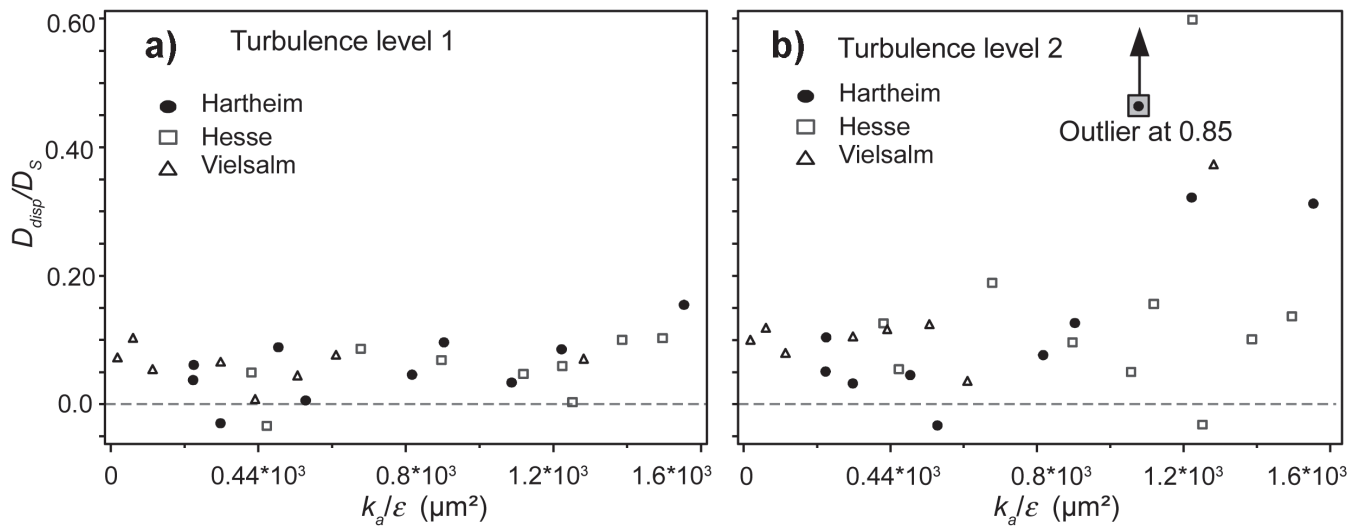


Fig. 8. Relationship between the ratio of gas transport processes (ratio of dispersion coefficient and effective diffusion coefficient, D_{disp}/D_S) and the parameter combination k_a/ϵ for (a) turbulence Level 1 and (b) turbulence Level 2. Negative D_{disp}/D_S values are due to measurement errors.

Both k_a and ϵ depend on the soil-water content and, hence, on soil matric potential. At Hartheim, the topsoil samples (0–5-cm depth) had high k_a/ϵ values and soil matric potential had only little impact (Fig. 9). The samples from Hesse revealed lower k_a/ϵ values at higher soil moisture, but the k_a/ϵ values were high. The Vielsalm samples generally had the lowest k_a/ϵ values that slightly increased when the soil was drier.

DISCUSSION

Laboratory Experiment

We could demonstrate the effect of turbulence-driven pressure pumping on gas transport in soil core samples through the activation of mechanical dispersion processes. Using the present set-up, it was possible to relate turbulence directly to the pressure-pumping effect and D_{disp} . The dispersion term, D_{disp} , is the product of the dispersivity, α , and the gas velocity in the soil pores ($D_{disp} = \alpha |\nu|$), which are parameters that are difficult to measure individually.

Until now, most of the experimental set-ups that have been used to measure α in the gas phase are based on the detection of the breakthrough curve of tracer gas when air is flowing

continuously through porous media (e.g., Poulsen et al., 2008; Hamamoto et al., 2009). However, these set-ups cannot be used to examine the pressure-pumping effect on the gas transport. We also wonder whether this α value corresponds to the α value for oscillating flow. Our set-up could also be adapted to field experiments to assess the impact of pressure pumping in the field, avoiding the determination of the individual parameters α and ν .

Over the three sites investigated, the parameter combination k_a/ϵ seems to be a suitable and physically-based surrogate to assess the sensitivity of gas transport in a soil to turbulence-driven pressure pumping. The relationship between k_a/ϵ and D_{disp} (Fig. 7) in soil samples with large ranges of pore sizes and structure shows that k_a/ϵ is the dominant soil property affecting the effectiveness of the pressure-pumping effect at the sample surface and agrees with predictions from the Massman (2006) model. In addition, our results show the need for accurate site-specific parameter determination. Simple models, which calculate k_a based on ϵ , already fix the relation between k_a and ϵ . However, this ratio can vary greatly between sites (Fig. 4). Therefore, we emphasize measurement instead of modeling the relevant soil physical parameters k_a , ϵ , and even D_S .

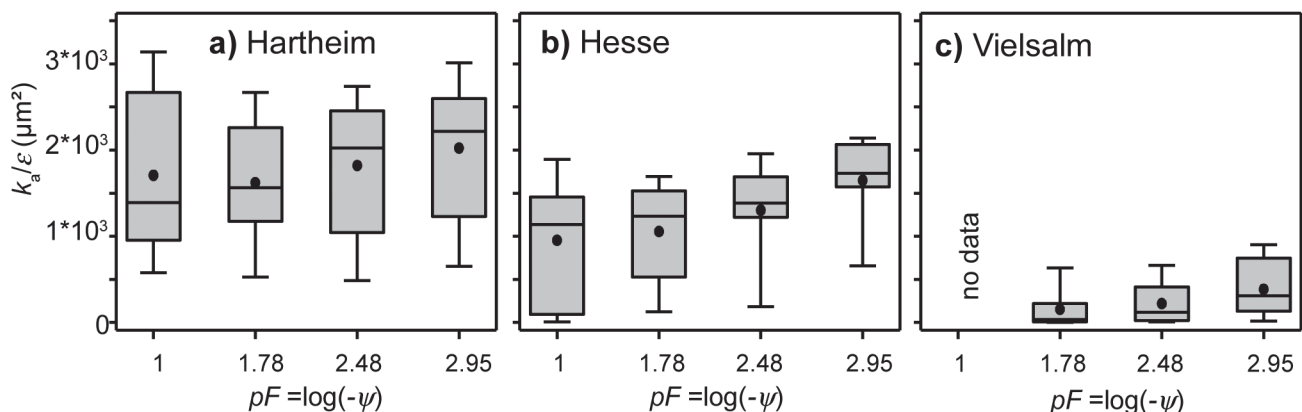


Fig. 9. Relationship between k_a/ϵ and pF of topsoil samples (0–5-cm depth), where k_a/ϵ is a surrogate for the susceptibility of a soil to pressure pumping, and pF the soil moisture status [$pF = \log(-\text{matric potential})$].

The turbulence-induced dispersive enhancement of the gas transport reached up to approximately 60% of the transport due to regular diffusion (D_{disp}/D_S). However, an enhancement >20% could only be observed at the higher turbulence level on samples with a $k_a/\varepsilon > 1000 \mu\text{m}^2$ (Fig. 8). Even though $1000 \mu\text{m}^2$ is very high for mineral soil, it is quite common for the humus layer. This threshold cannot be seen as a fixed value but rather depends on the intensity of the pressure pumping and the height of the sample. Hence, the uppermost few centimeters of the humus layer are always potentially affected by the turbulence effect.

The dispersivity α is an important parameter proportional to $D_{\text{disp}} (= \alpha \times v)$ at a given level of pressure pumping (Poulsen and Møldrup, 2006). It depends mainly on the geometry of the air-filled pores (Hamamoto et al., 2009), which is also influenced by soil moisture. Because k_a/ε can also depend on soil moisture (Fig. 8, see Hesse and Vielsalm), k_a/ε and α may covary negatively. Thus, higher soil-water content could lead to a lower k_a/ε value (Fig. 9) and probably also to higher α values (Costanza-Robinson and Brusseau, 2002). This could partly explain the relatively high D_{disp}/D_0 values of a Vielsalm samples at low values of k_a/ε , which exceed the modeled values (Fig. 7). Thus, modeling the pressure-pumping effect on soil gas transport could be improved using site-specific moisture dependence of k_a/ε and α .

The assumed amplitudes of the pressure fluctuations during our experiment were very low (0.5 Pa, 1 Pa). Yet, the observed increase in pressure fluctuations in the chamber below the soil sample agrees well with the assumed amplitudes and the dampening effect of the soil. These values can be considered realistic, although very low compared to values used in the synthetic datasets of Poulsen and Møldrup (2006) or those measured by Massman et al. (1997). In contrast, our measured k_a values were very high, so that even little pressure fluctuations had a substantial effect.

Relevance for Sites

Comparing the topsoil of the different sites, the samples from Hartheim showed the highest k_a values. This agrees with the high pore volume and the high fraction of macro/interaggregate pores (Fig. 3a). Soil moisture content has only little influence on k_a/ε (Fig. 9a), and, hence, this soil is sensitive to pressure pumping during all seasons. Because the values of k_a/ε are high throughout the profile, the pressure fluctuations can easily penetrate deeper into the soil. The penetrating depth is a very important factor. It represents the maximum depth to which the effect occurs. Additionally it affects directly the movement of the air column in the topsoil pores, since a deeper penetration depth means also a higher air-flow velocity in the topsoil pores. Another important issue is the transfer of turbulence above the canopy to the soil surface. At Hartheim the Scots pine canopy is sparse, and atmospheric turbulence can easily affect the soil surface. Therefore we have to expect a relatively large turbulence-driven pressure-pumping impact for this type of forest site during all seasons (e.g., Maier et al., 2010).

At the Hesse site k_a/ε (Fig. 9c), and thus D_{disp} at a given pressure fluctuation level, is generally lower. This means that the soil is less sensitive to pressure pumping than at Hartheim. Additionally, soil moisture has a more important influence. During summer the soil is drier leading to higher k_a/ε values and the soil gas transport becomes more sensitive to pressure pumping. However, the canopy of the beech stand is dense and only strong wind situations may induce turbulence near the forest floor. Poulsen and Møldrup (2006) suggested that turbulence-induced D_{disp} would become more important at higher soil moisture contents, because the relative contribution to the soil aeration (D_{disp}/D_S) increased. As a result, pressure pumping could be important at Hesse during winter, when the diffusivity is low.

At the Vielsalm site we expect atmospheric turbulence to have only little effect on soil gas transport, because k_a/ε is usually low (Fig. 9c). Especially during winter when there is no dense canopy the soil moisture is high and k_a/ε minimal. But also here pressure pumping could be important, since the diffusivity is also low.

To include turbulence-driven pressure pumping in field studies, precise information about the pressure fluctuation at the soil surface is needed. Additionally to the amplitude of the pressure fluctuation also wave frequency and wavelength is needed (Farrell et al., 1966; Kazanskiy and Zolotokrylin, 1994; Massman, 2006), which is difficult to measure. Seok et al. (2009), Massman and Frank (2006), and Bowling and Massman (2011) used wind speed as a surrogate for the pressure pumping, while Flechard et al. (2007), and Maier et al. (2010) used friction velocity u^* . Improvement could be made by studies linking u^* and high frequency pressure fluctuations at the soil surface, so wind data could be used to derive information about the pressure pumping. At forest sites, wind is usually measured above the canopy. But the transition of the above-canopy turbulence to pressure fluctuations at the soil surface must also be considered (Aubinet et al., 2003). Therefore we recommend to measure u^* above the soil surface as well. An approach to overcome the uncertainties from parametrization of D_S and D_{disp} would be to continuously measure the vertical profile of D_{res} in situ, similar to the radon method applied by Davidson and Trumbore (1995).

CONCLUSIONS

We showed how turbulence-driven pressure pumping can substantially enhance soil gas transport. We strongly recommend considering the turbulence effect on soil gas transport during field studies. The resulting diffusivity (D_{res}) should be used instead of the effective gas diffusion coefficient (D_S) for studies using the gradient method to measure soil gas efflux. Also efflux measurements using closed chambers are probably biased low compared with turbulence-driven pressure pumping in the field. Closing the chambers temporarily to measure the efflux probably excludes or attenuates the natural atmospheric pressure fluctuations. Hence, soil gas transport is modified and the efflux is probably lower when the chamber is closed.

ACKNOWLEDGMENTS

We would like to thank Flora Hofmann and Benjamin Eisele for their

assistance in the laboratory. Our thanks also go to Helmut Mayer for providing the sonic anemometer and technical assistance.

REFERENCES

- Amos, R.T., D.W. Blowes, L. Smith, and D.C. Segó. 2009. Measurement of wind-induced pressure gradients in a waste rock pile. *Vadose Zone J.* 8:953–962. doi:10.2136/vzj2009.0002
- Aubinet, M., B. Chermanne, M. Vandenhaute, B. Longdoz, M. Yernaux, and E. Laitat. 2001. Long term carbon dioxide exchange above a mixed forest in the Belgian Ardennes. *Agric. For. Meteorol.* 108:293–315. doi:10.1016/S0168-1923(01)00244-1
- Aubinet, M., B. Heinesch, D. Perrin, and C. Moureaux. 2005. Discriminating net ecosystem exchange between different vegetation plots in a heterogeneous forest. *Agric. For. Meteorol.* 132:315–328. doi:10.1016/j.agrformet.2005.08.006
- Aubinet, M., B. Heinesch, D. Perrin, and M. Yernaux. 2003. Horizontal and vertical CO₂ advection in a sloping forest. *Boundary-Layer Meteorol.* 108:397–417. doi:10.1023/A:1024168428135
- Bowling, D.R., and W.J. Massman. 2011. Persistent wind-induced enhancement of diffusive CO₂ transport in a mountain forest snowpack. *J. Geophys. Res.*, [Biogeosci.] 116:G04006.
- Clements, W., and M. Wilkening. 1974. Atmospheric pressure effects on ²²²Rn transport across the earth-air interface. *J. Geophys. Res.* 79:5025–5029. doi:10.1029/JC079i033p05025
- Costanza-Robinson, M.S., and M.L. Brusseau. 2002. Gas phase advection and dispersion in unsaturated porous media. *Water Resour. Res.* 28:1–10.
- Davidson, E.A., K. Savage, S.E. Trumbore, and W. Borken. 2006. Vertical partitioning of CO₂ production within a temperate forest soil. *Glob. Change Biol.* 12:944–956. doi:10.1111/j.1365-2486.2005.01142.x
- Davidson, E.A., and S.E. Trumbore. 1995. Gas diffusivity and production of CO₂ in deep soils of the eastern Amazon. *Tellus* 47B:550–565. doi:10.1034/j.1600-0889.47.issue5.3.x
- DeJong, E., and H. Schappert. 1972. Calculation of soil respiration and activity from CO₂ profiles in the soil. *Soil Sci.* 113:328–333. doi:10.1097/00010694-197205000-00006
- Delgado, J.M.P.Q. 2006. A critical review of dispersion in packed beds. *Heat Mass Transfer* 42:279–310. doi:10.1007/s00231-005-0019-0
- Elberling, B., F. Larsen, S. Christensen, and D. Postma. 1998. Gas transport in a confined unsaturated zone during atmospheric pressure cycles. *Water Resour. Res.* 34:2855–2862. doi:10.1029/98WR02037
- Fang, C., and J.B. Moncrieff. 1999. A model for soil CO₂ production and transport 1: Model development. *Agric. For. Meteorol.* 95:225–236. doi:10.1016/S0168-1923(99)00036-2
- FAO. 2006. World reference base for soil resources 2006. World Soil Resources Rep. 103. FAO, Rome.
- Farrell, D.A., E.L. Greacen, and C.G. Gurr. 1966. Vapor transport in soil due to air turbulence. *Soil Sci.* 102:305–313. doi:10.1097/00010694-196611000-00005
- Flechard, C., A. Neftel, M. Jocher, C. Ammann, J. Leifeld, and J. Fuhrer. 2007. Temporal changes in soil pore space CO₂ concentration and storage under permanent grassland. *Agric. For. Meteorol.* 142:66–84. doi:10.1016/j.agrformet.2006.11.006
- Fukuda, H. 1955. Air and vapor movement in soil due to wind gustiness. *Soil Sci.* 79:249–256. doi:10.1097/00010694-195504000-00002
- Gidda, T., D. Cann, W.H. Stiver, and R.G. Zytner. 2006. Airflow dispersion in unsaturated soil. *J. Contam. Hydrol.* 82:118–132. doi:10.1016/j.jconhyd.2005.09.005
- Granier, A., P. Biron, and D. Lemoine. 2000. Water balance, transpiration and canopy conductance in two beech stands. *Agric. For. Meteorol.* 100:291–308. doi:10.1016/S0168-1923(99)00151-3
- Granier, A., N. Breda, B. Longdoz, P. Gross, and J. Ngao. 2008. Ten years of fluxes and stand growth in a young beech forest at Hesse, North-eastern France. *Ann. For. Sci.* 65:704. doi:10.1051/forest:2008052
- Hamamoto, S., P. Moldrup, K. Kawamoto, T. Komatsu, and D.E. Rolston. 2009. Unified measurement system for the gas dispersion coefficient, air permeability, and gas diffusion coefficient in variably saturated soil. *Soil Sci. Soc. Am. J.* 73:1921–1930. doi:10.2136/sssaj2009.0012
- Hartge, K.H., and R. Horn. 1999. Die physikalische Untersuchung von Böden. 3rd ed. Ferdinand Enke Verlag, Stuttgart. (In German.)
- Hirsch, A.I., S.E. Trumbore, and M.L. Goulden. 2004. The surface CO₂ gradient and pore-space storage flux in a high-porosity litter layer. *Tellus* 56B:312–321. doi:10.1111/j.1600-0889.2004.00113.x
- Holst, J., R. Barnard, E. Brandes, N. Buchmann, A. Gessler, and L. Jaeger. 2008. Impacts of summer water limitation on the carbon balance of a Scots pine forest in the southern upper Rhine plain. *Agric. For. Meteorol.* 148:1815–1826. doi:10.1016/j.agrformet.2008.06.008
- Iversen, B.V., P. Schjønning, T.G. Poulsen, and P. Moldrup. 2001. In situ, on-site and laboratory measurements of soil air permeability: Boundary conditions and measurement scale. *Soil Sci.* 166:97–106. doi:10.1097/00010694-200102000-00003
- Jassal, R., T. Black, G. Drewitt, M. Novak, Z. Nestic, and D. Gaumont-Guay. 2005. Relationship between soil CO₂ concentrations and forest-floor CO₂ effluxes. *Agric. For. Meteorol.* 130:176–192. doi:10.1016/j.agrformet.2005.03.005
- Jiao, J.J., and H.L. Li. 2004. Breathing of coastal vadose zone induced by sea level fluctuations. *Geophys. Res. Lett.* 31:L11502. doi:10.1029/2004GL019572
- Kazanskiy, A.B., and A.N. Zolotokrylin. 1994. On the missing component in the equation for the land surface heat balance as applied to the heat exchange between the desert or semidesert surface and the atmosphere. *Boundary-Layer Meteorol.* 71:189–195. doi:10.1007/BF00709226
- Kühne, A., H. Schack-Kirchner, and E.E. Hildebrand. 2011. Gas diffusivity in soils compared to ideal isotropic porous media. *J. Soil Sci. and Plant Nutrition* 175(1):34–45. doi:10.1002/jpln.201000438.
- Maier, M., H. Schack-Kirchner, E.E. Hildebrand, and J. Holst. 2010. Pore-space CO₂ dynamics in a deep, well-aerated soil. *Eur. J. Soil Sci.* 61:877–887. doi:10.1111/j.1365-2389.2010.01287.x
- Massman, W.J. 2006. Advective transport of CO₂ in permeable media induced by atmospheric pressure fluctuations: 1. An analytical model. *J. Geophys. Res.* 111:G03004. doi:10.1029/2006JG000163
- Massman, W.J., and J.M. Frank. 2006. Advective transport of CO₂ in permeable media induced by atmospheric pressure fluctuations: 2. Observational evidence under snowpacks. *J. Geophys. Res.* 111:G03005. doi:10.1029/2006JG000164
- Massman, W.J., R.A. Sommerfeld, A.R. Mosier, K.F. Zeller, T.J. Hehn, and S.G. Rochelle. 1997. A model investigation of turbulence-driven pressure-pumping effects on the rate of diffusion of CO₂, N₂O, and CH₄ through layered snowpacks. *J. Geophys. Res.* 102:18851–18863. doi:10.1029/97JD00844
- Millington, R.J. 1959. Gas diffusion in porous media. *Science (Washington, DC)* 130:100–102. doi:10.1126/science.130.3367.100-a
- Moldrup, P., T. Olsen, T. Yamaguchi, P. Schjønning, and D.E. Rolston. 1999. Modelling diffusion and reaction in soil. IX. The Buckingham–Burdine–Campbell equation for gas diffusivity in undisturbed soil. *Soil Sci.* 164:542–551. doi:10.1097/00010694-199908000-00002
- Poulsen, T., and P. Moldrup. 2006. Evaluating effects of wind-induced pressure fluctuations on soil-atmosphere gas exchange at a landfill using stochastic modelling. *Waste Manage. Res.* 24:473–481. doi:10.1177/0734242X06066363
- Poulsen, T., W. Suwamarat, M.K. Hostrup, and P.N.V. Kalluri. 2008. Simple and rapid method for measuring gas dispersion in porous media: Methodology and applications. *Soil Sci.* 173:169–174. doi:10.1097/SS.0b013e31816408c9
- Pumpanen, J., H. Ilvesniemi, L. Kulmala, E. Siivola, H. Laakso, P. Kolari, C. Helenelund, M. Laakso, M. Uusimaa, and P. Hari. 2008. Respiration in boreal forest soil as determined from carbon dioxide concentration profile. *Soil Sci. Soc. Am. J.* 72:1187–1196. doi:10.2136/sssaj2007.0199
- Schack-Kirchner, H., E. Kublin, and E.E. Hildebrand. 2011. A finite-element regression procedure to estimate depth profiles of CO₂/N₂O production in soils. *Vadose Zone J.* 10:169–183. doi:10.2136/vzj2009.0193
- Scotter, D.R., and P.A.C. Raats. 1968. Dispersion in porous mediums due to oscillating flow. *Water Resour. Res.* 4:1201–1206. doi:10.1029/WR004i006p01201
- Scotter, D.R., and P.A.C. Raats. 1969. Dispersion of water vapor in soil due to air turbulence. *Soil Sci.* 108:170–176. doi:10.1097/00010694-196909000-00004
- Seok, B., D. Helmig, M.W. Williams, D. Liptzin, K. Chowanski, and J. Hueber. 2009. An automated system for continuous measurements of trace gas fluxes through snow: An evaluation of the gas diffusion method at a subalpine forest site, Niwot Ridge, Colorado. *Biogeochemistry* 95:95–113. doi:10.1007/s10533-009-9302-3
- Sharma, P., and T. Poulsen. 2010. Gas dispersion and immobile gas content in granular porous media: Effect of particle size nonuniformity. *Soil Sci.* 175:426–431. doi:10.1097/SS.0b013e3181f0edaf
- Soil Survey Staff. 2006. Keys to Soil Taxonomy. 10th ed. NRCS, Washington, DC.
- Stull, R.B. 1988. An introduction to boundary layer meteorology. Kluwer Acad. Publ., Dordrecht, the Netherlands.
- Takle, E.S., W.J. Massman, J.R. Brandle, R.A. Schmidt, X. Zhou, I.V. Litvina, R. Garcia, G. Doyle, and C.W. Rice. 2004. Influence of high-frequency ambient pressure pumping on carbon dioxide efflux from soil. *Agric. For. Meteorol.* 124:193–206. doi:10.1016/j.agrformet.2004.01.014